Biomechanics and Modeling in Mechanobiology (2024) 23:709–720
https://doi.org/10.1007/s10237-023-01801-7

ORIGINAL PAPER

The inclusion of the epithelium in numerical models of the human cornea

Andrea Montanino[1] · **Anna Pandolfi**[2]

Received: 2 October 2023 / Accepted: 27 November 2023 / Published online: 21 December 2023

Abstract
We present a patient-specific finite element model of the human cornea that accounts for the presence of the epithelium. The thin anterior layer that protects the cornea from the external actions has a scant relevance from the mechanical point of view, and it has been neglected in most numerical models of the cornea, which assign to the entire cornea the mechanical properties of the stroma. Yet, modern corneal topographers capture the geometry of the epithelium, which can be naturally included into a patient-specific solid model of the cornea, treated as a multi-layer solid. For numerical applications, the presence of a thin layer on the anterior cornea requires a finer discretization and the definition of two constitutive models (including the corresponding properties) for stroma and epithelium. In this study, we want to assess the relevance of the inclusion of the epithelium in the model of the cornea, by analyzing the effects in terms of uncertainties of the mechanical properties, stress distribution across the thickness, and numerical discretization. We conclude that if the epithelium is modeled as stroma, the material properties should be reduced by 10%. While this choice represents a sufficiently good approximation for the simulation of in vivo mechanical tests, it might result into an under-estimation of the postoperative stress in the simulation of refractive surgery.

Keywords Epithelium modeling · In-depth stromal stiffening · Nonlinear material models · Anisotropy · Finite elements

1 Introduction

The eye is a sequence of refractive lenses (cornea, aqueous humor, lens, vitreous humor), whose imperfections lead to the inability to focus objects. Because of its external position, the cornea is the surgeon's preferential site for the implementation of laser ablation refractive surgery, the clinical procedure used to correct vision defects by removing a portion of the corneal tissue and modifying the cornea shape.

From the mechanical point of view, the thinning of the corneal tissue may produce a non-negligible increase of the stress, a potential precursor of short- or long-term tissue degeneration (Sánchez et al. 2014; Simonini and Pandolfi 2015). While the optical changes induced by refractive surgery have been widely studied, alteration of the stress distribution due to geometrical modifications has received a relatively scant attention. The main motivations of this disinterest are the multiple uncertainties related to the definition of the mechanical properties of the corneal tissue, a heterogeneous, anisotropic, poro-viscous–elastic, and *patient-specific* material. The uncertainties related to the material and the impossibility to measure the physiological stresses, which can only be estimated by means of mechanical assumptions and numerical simulations, ravel the evaluation of the altered tissue engagement induced by the refractive surgery.

Most numerical investigations have been carried out to estimate the changes in the stiffness of the cornea after surgery (Sinha-Roy and Dupps 2009, 2011; Deenadayalu et al. 2006) or the variations in the stress field. Numerical studies document, in general, qualitative values of the stress

✉ Anna Pandolfi
anna.pandolfi@polimi.it

Andrea Montanino
andrea.montanino@unina.it

[1] Department of Structures for Engineering and Architecture, University of Naples "Federico II", Via Toledo 402, 80134 Naples, Italy

[2] Civil and Environmental Engineering Department, Politecnico di Milano, Piazza Leonardo da Vinci 32, 20133 Milan, Italy

distribution, with the objective of comparing preoperative and postoperative conditions. The comparison may become very difficult, since often the stress is reported in terms of the second invariant of the deviatoric stress (von Mises stress), a positive scalar which cannot discriminate between tensile and compression states and alter the perception of the actual tissue engagement (Sinha-Roy et al. 2014; Seven et al. 2017).

Indeed, the stress distribution is strictly related to the adopted material models and to their mechanical parameters, often grabbed uncritically from other studies and failing to be patient-specific (Pandolfi and Manganiello 2006). The most advanced models identify the material parameters through inverse analysis using data from ex vivo experiments (Sinha-Roy and Dupps 2011). Regrettably, the relation between ex vivo parameters and the corresponding in vivo values remains an unexplored patient-specific property. A few studies have tried to identify the mechanical properties by comparing preoperative and postoperative geometries (Sánchez et al. 2014; Simonini and Pandolfi 2015; Montanino and Pandolfi 2020), but the procedure is based on the knowledge of the postoperative geometry; thus, the methodology cannot be used to predict the mechanical response under surgery. In spite of all these difficulties, it is evident that the more a model is accurate in accounting for the microstructural features of the cornea, the more its predictions will be reliable.

The human cornea is a layered spherical shell, with an average thickness 558 to 580 μm, consisting in six layers. From the anterior surface, one finds: the corneal epithelium, made of five to seven cell layers, approximately 50 μm thick; the anterior basement membrane (ABM), about 50 nm thick; the Bowman membrane, in average 15 μm; the stroma, composed by collagen fibrils immersed in a matrix of proteoglycans and elastin, which can be 478 to 500 μm thick; the posterior basement membrane (or Descemet), about 10μm thick; and the mono-layer cellular endothelium, in average 5 μm thick. The second thickest layer of the cornea after the stroma is the epithelium.

Experimental studies documented a wide range of values for the elastic moduli of the stroma, with high differences due to the test type, experimental methodology, and type of cornea (human or animal). According to the values adopted in numerical studies, a realistic range of variability for the elastic modulus of the human stroma can be taken as 0.3-−0.6 MPa (Bryant et al. 2000; Jayasuriya et al. 2003).

The effective stiffness of the epithelium remains unknown. No direct (uniaxial tests, biaxial tests) measurements of the human epithelium stiffness have been reported in the literature, probably because of the impossibility to isolate the cellular layer from the supporting ABM. The exceedingly thin ABM layer possesses a compact structure that can be tested through atomic force microscopy (AFM): for the elastic modulus of ABM, the value 7.5±4.2 kPa has been reported in Last et al. (2009). Yet, the epithelium must be able to offer some shear stiffness, since it is exposed to—and has to react to—different types of mechanical stimuli: the shear stress from the tear film motion and blinking, the extracellular matrix interaction, and external physical forces such as eye rubbing and contact lens wear (Masterton and Ahearne 2018). A subsequent AFM-based study, where anisotropy and the inhomogeneity of the tissues have been considered, estimated the average elastic modulus for several corneal layers, and reported for the stroma the rather low average value of 33.1±6.1 kPa (Last et al. 2012). For human corneas, they concluded that the stiffness ratio between ABM and stroma was 23%.

For the sake of comparison, a study involving AFM measurement on rabbit corneas reports the both values for the elastic modulus of epithelium and stroma (Thomasy et al. 2014). Absolute values have no correspondence with human corneas, since not only they are about two orders of magnitude smaller, but the microstructure of the rabbit stroma is known not to be characterized by the presence of interlacing collagen lamellae. In Thomasy et al. (2014), the elastic modulus as determined by AFM was 0.57±0.29 kPa for epithelium, 1.1±0.5 kPa for anterior stroma and 0.38±0.22 kPa for posterior stroma (average 0.74±0.26 kPa). For rabbit corneas, the stiffness ratio between epithelium and stroma was 77%, which disagrees with observations in humans.

In the lack of experimental evidence on the epithelial corneal tissue, some significant estimate of the elastic modulus can be obtained from AFM measurements on single epithelial corneal cells. In Straehla et al. (2010), an indentation model that modeled a single cell as a spring bed estimated the Young's modulus of the epithelial corneal cell as 16.5±8.83 kPa. A more recent study Bongiorno et al. (2016) reports for the Young's modulus of the single epithelial corneal cell a value one order of magnitude smaller, i.e., 1.7 kPa. Thus, an indicative interval of variability for the Young's modulus of the corneal epithelium can be taken as 1.7–25 kPa.

In the shortage of data relevant to the thinner layers, numerical simulations have been disregarding the five layers of the cornea, and model a single tissue by extending the mechanical properties of the central stroma to the all layers. However, previous studies demonstrated that modeling the layered structure of the bovine cornea in terms of epithelium, stroma and endothelium has a rather important relevance on the mechanical response (Elsheikh et al. 2009), while the Bowman layer seems to play a minor role (Torres-Netto et al. 2021).

Advanced optical instruments used in the current practice (e.g., optical coherent tomography, OCT) provide the patient-specific geometry of the cellular layers of the cornea, which suggests to reconsider the inclusion of the epithelium

in numerical applications. The inclusion of the epithelium in the cornea model has significance under two points of view. First, the correct estimation of the stresses requires the description of the epithelium, otherwise the stresses in the stroma are underestimated and stress discontinuities cannot be detected. Second, in the perspective of modeling refractive surgery, with ablation of the anterior layers of the cornea, the presence of the epithelium is fundamental to reproduce the actual changes in the geometry of the cornea and predict the temporary engagement of the tissues. The goal of the present study is to assess the role of the epithelium in the mechanical response of a cornea model to the physiological action of the intraocular pressure (IOP). We are interested in quantifying the under-estimation of the stress when the epithelium stiffness is incorporated in the stromal stiffness. Numerical simulations show that the stress peaks in the stroma can be actually 10% larger than what estimated in absence of the epithelium.

The paper is organized as follows. In Sect. 2, we quantify the relevance of the epithelium on the global stiffness of the cornea by using a simplified linearized shell model. Next, we focus on the patient-specific model described in Montanino et al. (2023), extended in order to include the epithelium and discretized into finite elements. In Sect. 3, using finite element simulations, we establish the dependence of the global stiffness of the cornea, main responsible of the global biomechanical response, on the ratio between the epithelium and stroma stiffness. In Sect. 4, we discuss the characteristics of proposed model focusing on the advancement of the knowledge and on the potential of improvement of numerical corneal models.

2 Materials and methods

This study clearly applies to patient-specific geometries, characterized by corneal layers of variable thickness. Nevertheless, before starting to conduct numerical analyses that account for the complex structure of the cornea, we want to acquire a quantitative awareness on the influence of the direct modeling of the epithelium on the 'equivalent' mechanical properties of the stroma. This estimate leads to the definition of upper- and under-bounds for the homogenized elastic modulus of the cornea to be used in simple applications where la cornea is assumed to be homogeneous. These applications are still common in the literature because of the rapid numerical response. By comparison with the results of more advanced models, such bounds will also be useful in assessing the limitations of linear models.

We begin with a simplified mechanical equivalent of the cornea that captures the interplay between stiff and compliant layers. In the simplified model, the material is assumed to be linear elastic and characterized by a variable elastic modulus $E(z)$, where z is a coordinate across the corneal thickness with origin at the posterior surface. We compare the behaviors of layered and homogeneous materials by assuming that the cornea is uniformly elongated. In the following derivation, we neglect the posterior layers (Descemet and endothelium) because of their small thickness and their scarce or null relevance in refractive surgery procedures.

2.1 Estimate of corneal stiffness bounds

While for complex material models the material stiffness is the result of the combination of several contributions, for linear elastic material models the material stiffness can be identified with the elastic moduli. The elastic moduli reported in literature studies for linear elastic model of the cornea are in the range 300–600 kPa, cf, e.g., Bryant and McDonnell (1996), Cabrera Fernandez et al. (2005). As mentioned in introduction, the few experimental data on corneal epithelium stiffness locate the Young's modulus in the range 1.7–25 kPa, a value a few orders of magnitude smaller than the average stiffness of the stroma reported in the literature. The comparison between these two ranges minimizes the mechanical relevance of the epithelium, while it undoubtedly contributes to the geometry of the thickness (and, to some extent, to the refractive power).

Before starting the numerical calculations, we begin by deriving some bounds for the stiffness of the composite made by epithelium and stroma.

We denote with t_e and t_s the thickness of the epithelium and of the stroma, respectively. The total thickness is $t = t_e + t_s$, see Fig. 1a. The epithelium thickness is a small percentage q of the corneal thickness, i.e.,

$$t_e = q\,t\,, \qquad t_s = (1-q)\,t\,. \tag{1}$$

The elastic modulus of the epithelium E_e can also be expressed as a percentage Q of the average elastic modulus of the stroma E_s as

$$E_e = QE_s. \tag{2}$$

Let us now account for the variability of the normal elastic modulus E across the thickness. The simplest assumption is a piece-wise-constant distribution, see Fig. 1b, where the elastic modulus of the stroma E_s is constant, we obtain the equivalent elastic modulus of the cornea E_c as

$$E_c = \frac{E_e t_e + E_s t_s}{t} \tag{3}$$

Through Eqs. (1)-(2), Eq. (3) becomes

$$E_c = (1 - q + qQ)E_s \tag{4}$$

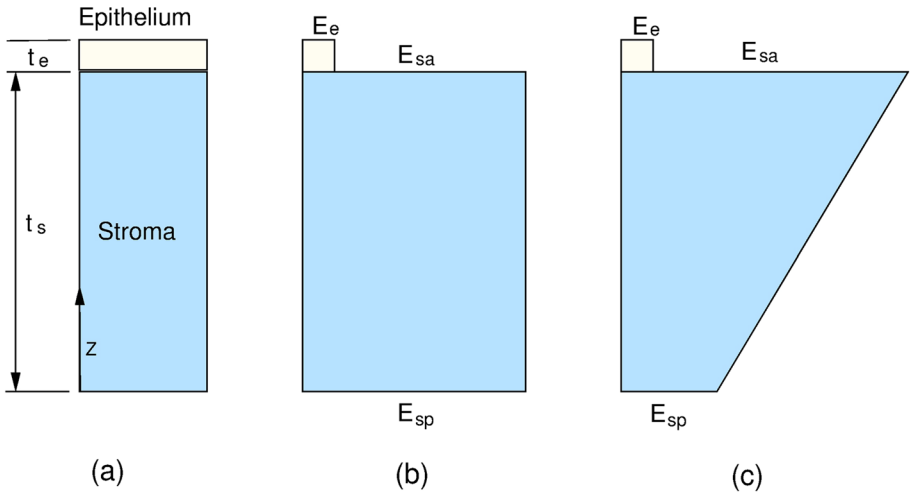

Fig. 1 Assumptions on the distribution of the normal elastic modulus across the thickness of the cornea. **a** Geometry of a thin portion of the cornea taken at the apex, with $t = t_e + t_s$, where the anterior basement membrane is considered integrated into the epithelium. **b** Piecewise constant distribution of the normal elastic modulus across the thickness. **c** Linear distribution of the elastic modulus in the stroma and constant distribution in the epithelium

Since the average values of stroma and epithelium thickness are known, we can take $0.0862 \le q \le 0.0896$. Applying the two limiting values for the ratio $0.03 \le Q \le 0.08$ leads to

$$0.903E_s \le E_c \le 0.911E_s\,, \tag{5}$$

$$1.097E_c \le E_s \le 1.107E_c\,. \tag{6}$$

If we assume a linear distribution for the elastic modulus in the stroma, see Fig. 1c, we identify with E_s the average stiffness of the stroma. Since the anterior stroma elastic modulus E_{sa} is several times larger than the posterior stroma elastic modulus E_{sp}, we write $E_{sa} = mE_{sp}$, and

$$E_s = \frac{1+m}{2}E_{sp} = \frac{1+m}{2\,m}E_{sa} \tag{7}$$

An acceptable estimate $m \approx 3$ can be derived from tests on the shear stiffness of the stroma, cf. Petsche and Pinsky (2013),

$$1.806E_{sp} \le E_c \le 1.822E_{sp}\,, \tag{8}$$

or

$$0.602E_{sa} \le E_c \le 0.607E_{sa}\,. \tag{9}$$

These relations define a reliable estimate of the lower- and upper-bounds to assign to the stroma, in the eventuality that some experimental information of the corneal stiffness is available.

2.2 Finite element model

In numerical calculations, we use a finite element code developed in house, whose details have been reported elsewhere (Pandolfi and Manganiello 2006; Simonini and Pandolfi 2015; Montanino et al. 2018, 2023). The code performs static and dynamic analyses of patient-specific geometries of the human cornea under the action of the IOP (Pandolfi and Manganiello 2006; Simonini and Pandolfi 2015) or other typical mechanical test (Montanino et al. 2018, 2019), and evaluates the postoperative behavior after refractive surgery (Sánchez et al. 2014; Montanino et al. 2023). The boundary conditions account, with proper kinematics, for the missing tissues (sclera and iris). The equilibrium equations are solved by a fully explicit approach, which sees the static solution as the steady state of a critically damped dynamic problem. The code acquires the patient-specific geometries of the patients from diagnostic images, and is equipped with a large number of material models for the stroma. The most sophisticated material model accounts for inhomogeneity and anisotropy by describing through a semi-stochastic model (Pandolfi and Vasta 2012) the micro-architecture of reinforcing collagen according to X-ray observation (Meek and Boote 2009). A quick reminder of the material model is reported in Appendix A.

We use a unique patient-specific geometry, chosen among the ones examined in Montanino et al. (2023). The geometry of the patient-specific cornea is obtained from the three-dimensional images of a corneal topographer. The instrument segments automatically the tissues of the cornea returning three sets of points describing the anterior surface, the posterior surfaces, and the interface between epithelium and stroma. The points are projected on a plane orthogonal to the optic axis of the eye to define the extension of the cornea within an ellipse. The ellipse is subdivided into four-edge polygons, according to a topological mapping that follows the main orientation of the collagen fibrils: orthogonal in the center, circumferential, and radial at the limbus (Pandolfi and Manganiello 2006). The nodes of the polygons are then projected back onto the anterior, posterior, and epithelium surfaces, along lines orthogonal to the surfaces. Furthermore, the stroma is subdivided in

several layers across the thickness. The spatial disposition of the nodes allows to define eight-noded brick elements with a smooth variation of the shape toward the limbus. The mapping has been conceived to provide a very regular subdivision in the optical zone, where the accuracy of the discretization is most important.

Since the mechanical properties are variable across the thickness, we consider six levels of discretization, see Table 1, progressively increasing the number of stromal layers and, accordingly, reducing the meridian size of each element. Figure 2 shows the coarsest (1) and finest (6) meshes. Note that the patient-specific geometry is not axis-symmetric. Three meshes (1, 3, and 5) consider the cornea made exclusively of stroma. Three meshes (2, 4, and 6) include the model of the epithelium. In this case, the epithelium layer is constructed on the patient-specific data, thus it is identical in the three meshes, while the stroma is subdivided, respectively, in 3, 6, and 9 layers of equal thickness.

The reference material properties for this study have been calibrated in simulations of refractive surgery and mechanical tests on human eyes, reported in previous works of our group (Sánchez et al. 2014; Simonini and Pandolfi 2015; Montanino et al. 2018). As explained in Appendix A, the stiffness parameters of the model are seven, five stiffness coefficients and two dimensionless rigidity coefficients. We assume a linear variation of the parameters from the posterior to the anterior sides of the cornea, according to the values listed in Table 2. For the models with no epithelium, the variation includes the corneal thickness (first two lines in Table 2). For the models with the epithelium, the variation ends at the interface between stroma and the epithelium (first two lines in Table 2). According to the consideration of the previous section, the stiffness coefficients of the cornea (considered as a 'homogeneous' tissue) are about 10% less than the ones of the stroma (considered as 'layered' tissue).

Each layer of the model has been characterized with the set of material parameter values corresponding to the position of the barycenter of each element belonging to the layer, according to a linear interpolation between posterior and anterior surfaces. The values of the parameters at the anterior and posterior surfaces are reported in Table 2.

For the meshes 2, 4, and 6, the epithelium is modeled as a NeoHookean material extended to the compressible range, characterized by a bulk modulus K_e and a shear

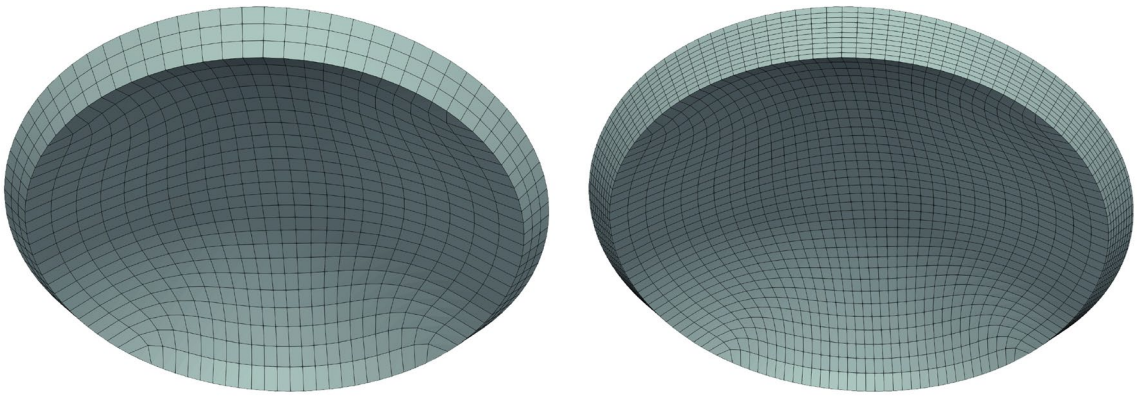

(a) Mesh 1 (b) Mesh 6

Fig. 2 Two of the six meshes used in the numerical simulations. **a** Coarsest mesh, no epithelium, comprising 1,728 elements and 2,500 nodes, **b** Finest mesh, with epithelium included, comprising 11,560 elements and 13,475 nodes. The anterior layer represents the epithelium

Table 1 Finite element discretization of the patient-specific cornea used in the study, including six different models

No.	Elm NT	Elm SI	Elm Th	Elm Epi	Elements	Nodes	Time [min]
1	25	25	3	0	1728	2500	18
2	25	25	4	1	2304	3125	19
3	30	30	6	0	5046	6300	82
4	30	30	7	1	5887	7200	97
5	35	35	9	0	10,404	12,250	248
6	35	35	10	1	11,560	13,475	278

Elm NT: elements across the nasal–temporal meridian. Elm SI: elements across the superior–inferior meridian. Elm Th: element across the thickness. Elm Epi: elements across the epithelium. Elements: number of eight-noded brick elements. Nodes: number of nodes. Time: average computational time requested for the full analysis in a single core execution

Table 2 Material properties used for the corneal tissue, according to the distributed fiber model adopted (Appendix A)

Epi	Side	K [MPa]	μ_1 [MPa]	μ_2 [MPa]	k_{11} [MPa]	k_{12}	k_{21} [MPa]	k_{21}
No	Post	5.5	0.036	− 0.009	0.023	91	0.023	91
No	Ant	5.5	0.109	− 0.027	0.068	273	0.068	273
Yes	Post	5.5	0.04	− 0.01	0.025	100	0.025	100
Yes	Ant	5.5	0.12	− 0.03	0.075	300	0.075	300
No/Yes	Uni	5.5	0.08	− 0.02	0.050	200	0.050	200

The table reports the material parameter values at the anterior and posterior surface of the stroma, which vary linearly across the thickness. Lines 1–2 refer to the cornea as a single homogeneous layer; lines 3-4 refer to the stroma when separated from epithelium. Line 5 refers to the material used for the test of convergence in a homogeneous model

Table 3 Material properties used for the epithelium tissue, treated as a NeoHookean hyperelastic material

Epi	K_e [MPa]	μ_e [MPa]	E_e [MPa]	ν_e
Ref	1.53	1.58	0.46	0.45
0.1	0.153	0.158	0.046	0.45
0.05	0.0153	0.0158	0.0046	0.45
0.01	0.00153	0.00158	0.00046	0.45

Line 1 reports the values to be assigned to obtain a NeoHookean material with a stiffness equivalent to the one of the fiber reinforced material used for the stroma. Lines 2-4 report the values adopted in the numerical calculations

modulus μ_e. In the simulations, we considered different values of the corresponding Young's modulus E, by keeping $\nu = 0.45$ constant, see Table 3. Note that the first line of Table 3 reports the elastic parameters of a NeoHookean material with a stiffness equivalent to the one of the fiber reinforced material used for the stroma, i.e., E_e =460 kPa. This value falls in the 300–600 kPa range typically used in numerical studies of the cornea.

For each model, the unstressed geometry of the cornea has been identified with the iterative procedure described in Pandolfi and Manganiello (2006), by assuming 16 mmHg for the physiological IOP. The procedure is strongly related to the chosen material model and the chosen parameters, thus the retraction of the unstressed cornea with respect to the physiological configuration differs according to the parameters as well as to the finite element discretization, in consideration of the nonlinearities involved (kinematics and materials). Thus, results in terms of displacement field are affected by the identification process, since the coordinates of the models will be different at the unstressed state but they have to coincide at the physiological IOP. This will introduces a shift between global responses in the apex displacement versus IOP plots.

3 Results

The analyses simulate the pressurization of the cornea with an increasing IOP, from 0 to 30 mmHg. A preliminary analysis set was conducted by adopting the same mechanical properties for all the layers, including the epithelium, to perform a convergence analysis, showing that all the meshes provided a very similar response. In the subsequent analyses, the difference in the number of layers has been exploited to assess the relevance of the inclusion of a thin layer in the models. In all the simulations, the material properties vary linearly across the thickness, as specified in Table 2.

Results are presented in terms of displacements (global curves IOP versus apex displacement, and distribution of optic axis displacement component), and stresses (distribution of the normal component of the Cauchy stress in the meridian nasal–temporal, NT, direction).

The IOP versus apex displacement curves are useful to provide a synthetic indication of the mechanical response of the cornea, and are often used in the literature to characterize its stiffness. The slope of the curve is a measure of the global stiffness of the tissue that depends on the stiffness of the epithelium and of the stroma.

Figure 3 compares the IOP–apex displacement curves for the three models (1, 3, and 5) that model only the stroma. The finest mesh shows a stiffer behavior, while the intermediate and coarse meshes provide a very similar response.

Figure 4 compares the curves for the three models (2, 4, and 6) that model the stroma and the epithelium, with the epithelium characterized by mechanical properties equivalent to the average stiffness of the cornea, see line 1 of Table 3, i.e., inferior to the stiffness of the adjacent stroma. In this case, the stiffest behavior is offered by the coarse mesh, while the intermediate and the fine meshes show a similar response. The comparison between Figs. 3 and 4 shows that the introduction of an extra layer with an average stiffness modifies substantially the mechanical response of the cornea.

The discrepancy between the trend shown by the two plots can be explained as follows. A linear variation of

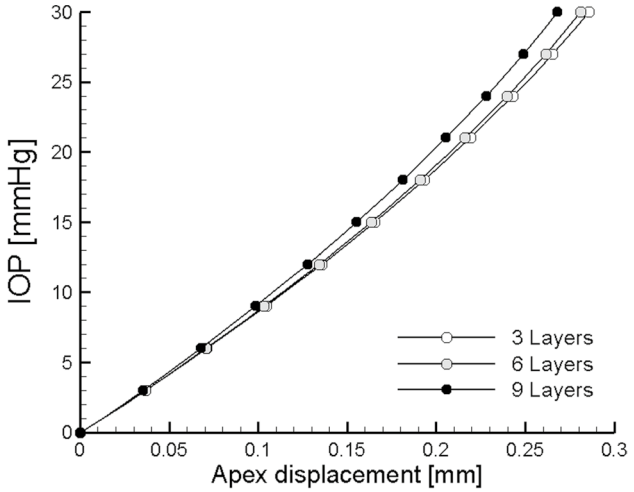

Fig. 3 IOP versus apex displacement curves. Comparison between models considering only the stroma

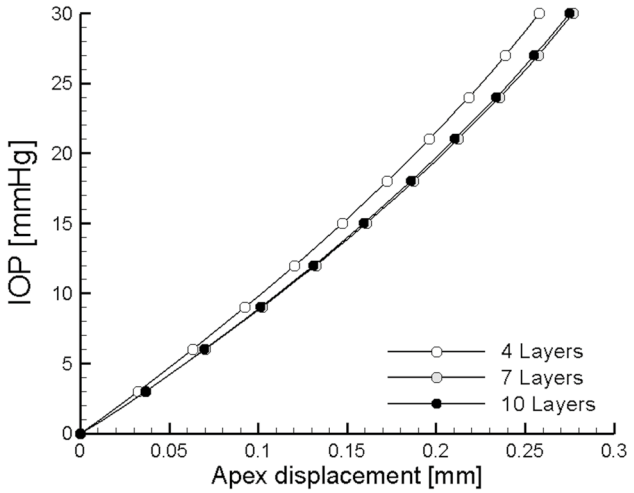

Fig. 4 IOP versus apex displacement curves. Comparison between models including an extra layer as epithelium, but assigning properties equivalent to the average stiffness of the stroma

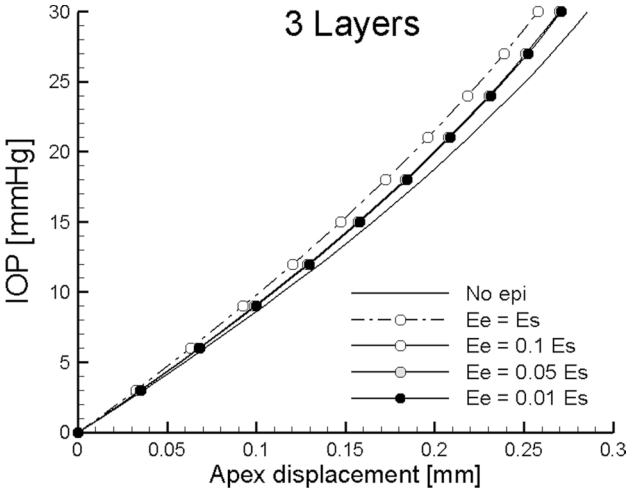

Fig. 5 IOP versus apex displacement curves, influence of the epithelium stiffness on the mesh with three stroma layers. Plots include the model of the sole stroma (solid lines), and the models with epithelium. Broken line: epithelium with stroma stiffness. Solid lines with symbols: epithelium with reduced stiffness

the mechanical properties in the stroma implies that each element is characterized by the material properties corresponding to its barycenter. If thinner layers are adopted, the material stiffness of the outermost layer becomes higher, providing a global increment of the corneal stiffness with respect to thicker layers. If the epithelium is included (using for it the stiffness of the mid-stroma), the outermost layer remains always characterized by a reduced stiffness, introducing a nonlinearity in the distribution of the stiffness across the thickness. The nonlinearity justifies the inversion of the mechanical response between the three discretizations with respect to the case without epithelium.

Figure 5 compares the curves for models 1 and 2 that include three layers for the stroma. The plot visualizes the effect of the presence of the epithelium, starting from the case where the epithelium is assigned a stiffness equivalent to the average stroma stiffness, and reducing the stiffness to 10%, 5% and 1% of the stroma stiffness.

The plot says that the contribution of the epithelium to the global stiffness of the cornea is negligible. In fact, a reliable value of the stiffness of the epithelium cannot be superior to 10% of the stiffness of the stroma. With the maximum stiffness of the epithelium, the cornea is more compliant than when composed only by stroma. The reduction of the stiffness of the epithelium to smaller values does not modifies the mechanical response of the cornea, since the curves are practically superposed.

Similarly, Figs. 6 and 7 compare the curves for models 3 and 4—including six stromal layers—and models 5 and 6—including nine stromal layers, respectively. Results confirm the behavior observed for the models with three layers. Figure 8 compares the distribution of the component of the displacement in the direction of the optic axis along the NT meridian of the cornea for the six discretizations. For the models with epithelium, the results are shown for the case $E_e = 0.05E_s$. Figure 9 compares the normal NT Cauchy stress distribution across the NT meridian for the six discretizations; for the models with epithelium, the results are shown for the case $E_e = 0.05E_s$. The maximum and minimum values of the normal Cauchy stress in the NT direction on the meridian NT section are collected in Table 4.

The average execution times for the analyses are listed in the last column of Table 4. With respect to the coarsest mesh, the computational time of the middle size mesh

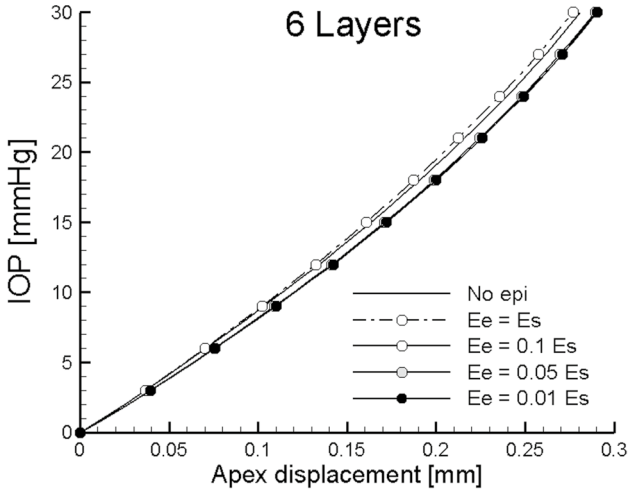

Fig. 6 IOP versus apex displacement curves, influence of the epithelium stiffness on the mesh with six stroma layers. Plots include the model of the sole stroma (solid lines), and the models with epithelium. Broken line: epithelium with stroma stiffness. Solid lines with symbols: epithelium with reduced stiffness

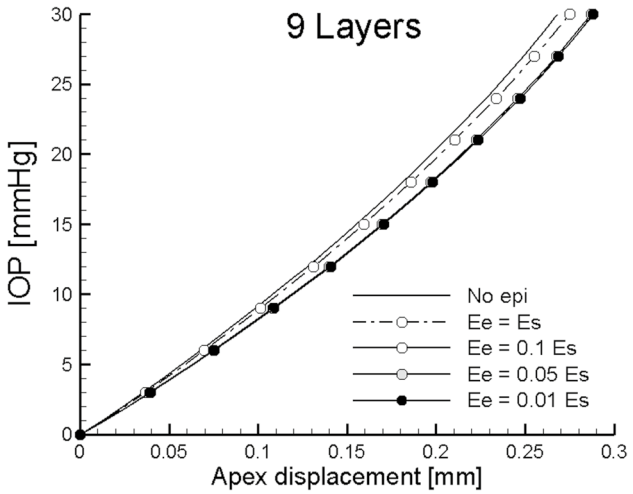

Fig. 7 IOP versus apex displacement curves, influence of the epithelium stiffness on the mesh with nine stroma layers. Plots include the model of the sole stroma (solid lines), and the models with epithelium. Broken line: epithelium with stroma stiffness. Solid lines with symbols: epithelium with reduced stiffness

requires is 5 times longer and the finest mesh 15 times longer.

4 Discussion

The layered structure of the cornea is often disregarded in numerical simulations, because of the mechanical predominance of the stroma over the other layers (Cabrera Fernandez et al. 2005; Alastrué et al. 2006; Studer et al. 2013; Elsheikh et al. 2015; Whitford et al. 2015; Ariza-Gracia et al. 2017). By the way of simplification, the mechanical properties of the stroma are simply extended to the thinner layers, and the material is considered homogeneous. Even in sophisticated models where a variability across the thickness is assumed (Montanino et al. 2018), the epithelium is in general disregarded. In support of this choice, there are several well founded reasons. First of all, the mechanical properties of the thinner layers (epithelium, Bowmann, Deshmet, and endothelium) have never been measured in humans. Furthermore, their exceeding small thickness requires a refinement of the mesh also in the meridian direction, with a disproportionate increase of the computational cost.

In the recent literature, an exception to this common way to proceed is represented by an interesting study on the biomechanics of the keratoconus, where the authors model the thin layers with the goal to capture the conditions that lead to the formation of a conus in a diseased cornea (Falgayrettes et al. 2023). Regrettably, the selection of the material properties of the thin layers is not commented or justified; also the discretized finite element model adopted in the numerical simulation is not shown.

Despite the common belief that the corneal epithelium is mechanically non-relevant, it actually plays a role in the mechanical stiffness of the cornea, because it counts for about the 10% of the total thickness. Under the assumption that the cornea behaves as a homogeneous material, with uniform properties across the thickness, the stiffness of the stroma must be reduced in order to compensate the increased thickness. This means that a corneal model without epithelium must be characterized by smaller mechanical properties with respect to a non-homogeneous model. A reduction of the mechanical properties leads, for the same deformation of the system, to a proportional reduction of the stress, that can be underestimated.

The analysis of the influence of the epithelium on the mechanical response of the cornea has been carried out in this study by considering a sophisticated nonlinear material model of the stroma that accounts for the presence of collagen reinforcement, see Appendix A. The architecture of the collagen reflects the findings of the X-ray analyses of post-mortem corneas (Agca et al. 2014). Furthermore, in this study a variation of the stiffness across the thickness, with a ratio 3/1 between anterior and posterior stromal stiffness, has been considered (Montanino et al. 2018). This choice is consistent with the anatomy of the cornea, since the epithelium is resting on the stiffest portion of the stroma.

The presence of a stiffness gradient across the thickness raises questions on the discretization. In the standard finite element approach, each element is characterized by a unique material. In the present model, each eight-noded brick element has eight integration points, and the orientation/

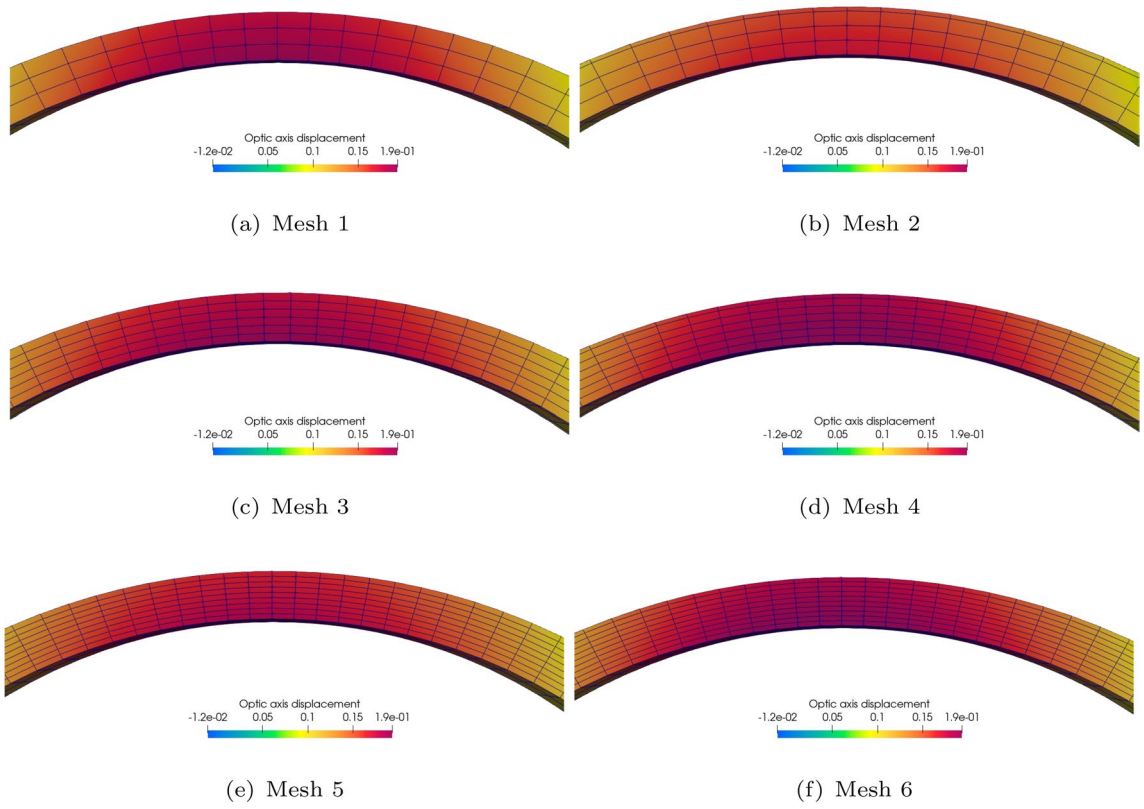

Fig. 8 Distribution of the displacement component in the optic axis direction across the NT meridian of the cornea. On the left columns, the models without epithelium. On the right column, the models with epithelium and $E_e = 0.05E_s$

dispersion of the collagen fibrils is variable according to the depth. However, the material properties in each element are the same for the eight integration points. This implies that a discretization refinement in the thickness will provide a more accurate description of the stiffness gradient. Note that the geometrical and material nonlinearities will alter the convergence of the model with the reduction of the mesh size, which is instead observed in homogeneous and uniform cases.

To preserve good properties of convergence, the elements of a mesh must have a good aspect ratio, i.e., a refinement of the mesh in the thickness must be accompanied by a refinement of the mesh along the meridian direction. The typical discretization used in previous studies (with no property gradient across the thickness) considered three layers for the thickness. Results were satisfactory except for loads that caused the change of the concavity of the cornea, e.g., indentation and air puff tests (Montanino et al. 2018). In the present study, three layers seems to be insufficient to describe the behavior of the tissue. This observation is confirmed by the IOP versus apex displacement plots of Fig. 5. The mechanical response of the three-layer model (solid line) and the four-layer model, inclusive of the epithelium with a stiffness corresponding to the average stiffness of the stroma (broken line with white circles), are very different. The latter is stiffer, revealing that the inclusion of a thin layer on top of thick layers leads to an unsatisfactory result, albeit expected. Contrariwise, both the six-layer and nine-layer models are sufficiently precise: the mechanical response of the sole stroma and of the epithelium inclusive models are very similar, see the solid lines versus the broken lines in Figs. 6 and 7. The anomalous behavior of the coarse model is also confirmed by the comparison of Figs. 3 and 4, which reveal an inversion of the stiffness trend with the mesh refinement: for the pure stroma models, the coarse mesh shows a softer behavior, while for the epithelium models, the coarse mesh shows a stiffer behavior. As already mentioned, the discrepancy is due to the presence of a thickness gradient in the material properties.

The most interesting part of the study is related to the quantification of the epithelium stiffness relative to the stroma stiffness. The absence of experimental data has to be ascribed to the very low values of the epithelium stiffness which makes it impossible to evaluate them. A simple yet correct observation is that the epithelium must have a stiffness one or two orders of magnitude inferior to the stroma stiffness. Here we consider three different values of the epithelium stiffness, 10%, 5% and 1% of the average stoma

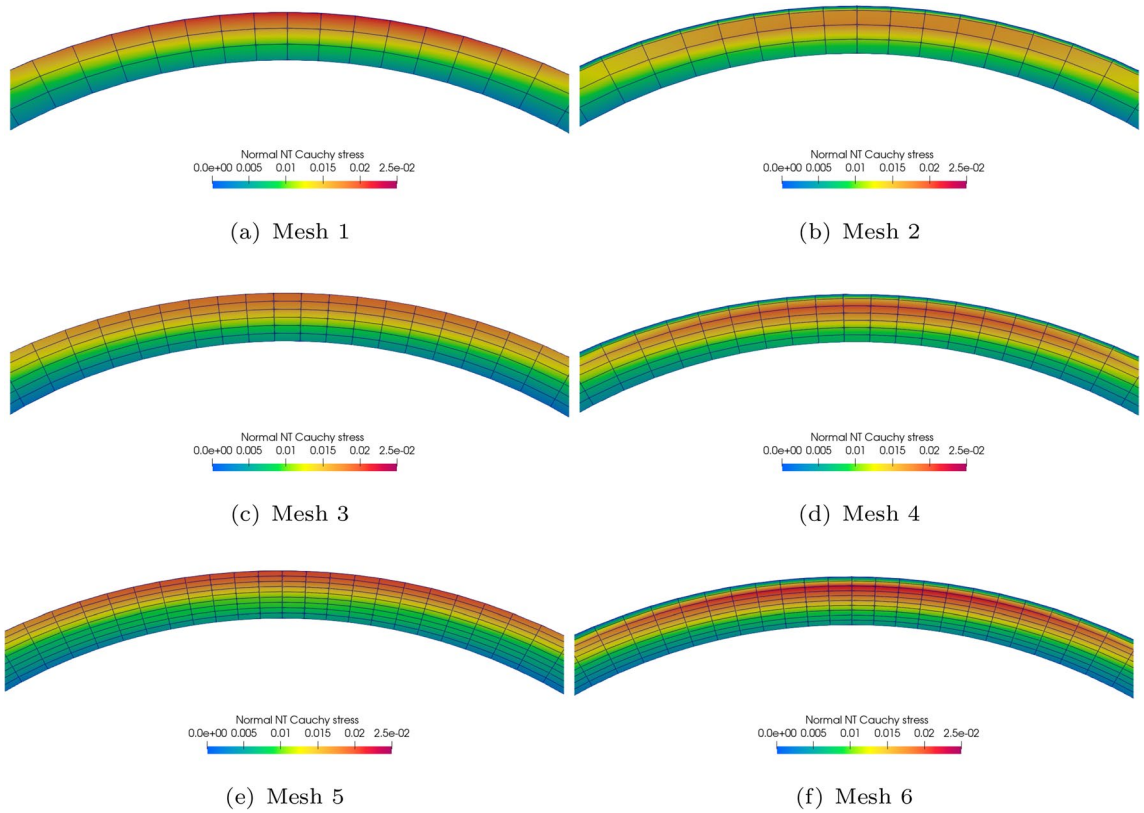

Fig. 9 Distribution of the normal component in the NT direction of the Cauchy stress, across the NT meridian of the cornea. On the left columns, the models without epithelium. On the right column, the models with epithelium and $E_e = 0.05E_s$

stiffness. Numerical analyses reveal that the actual value of the epithelium stiffness, if below 10% of the stroma stiffness, does not affect the global mechanical response of the cornea in terms of displacements, see Figs. 5, 6, and 7, solid curves with white, gray and black circles, as well as of stresses. In all the discretizations, though, the mechanical response for the model inclusive of a soft epithelium differs from the one where only the stroma is accounted for.

An additional observation is that the displacement field is very similar for all the models, see Fig. 8. As matter of fact, under the action of the IOP the dominant displacement component is the one in the direction of the optic axis, and no appreciable difference can be observed between the models.

Table 4 Maximum and minimum normal stresses in the NT direction for the six models

No	Max σ_{NT} [kPa]	Min σ_{NT} [kPa]	Time [min]	Rel cost
1	22	4.5	18	1.00
2	17	1.4	19	1.05
3	19	4.8	82	4.55
4	20	3.0	97	5.38
5	20	5.1	248	13.77
6	22	2.9	278	15.44

Contrariwise, the stress profile across the thickness shows large differences between the models, see Fig. 9. In the epithelium models, the maximum stress is observed in the anterior stroma layer, while the stress in the epithelium is at least one order of magnitude smaller than the stress in the stroma. This behavior is due to the difference in stiffness between the two tissues: at the same strain, the stress is roughly proportional to the stiffness of the material. In the pure stroma models, instead, the stress follows the material property gradient. With the exception of the three stroma layer models, the stress in the models with epithelium is 5–10% larger than in the models without epithelium. Interestingly, the increment of the stresses is strictly related to the increment of the material properties, in turn associated to the reduction of the effective thickness.

The 10% stress increment in the anterior layers of the cornea due to the presence of the softer epithelium, as revealed by the models here analyzed, is *de facto* always present in the anterior stroma, because in the natural cornea the epithelium is there. A 10% larger stress will be observed also in models, when accounting for the epithelium, that simulate

the cornea after refractive surgery, see, e.g., Montanino et al. (2023). This moderate increase of the stress due to the inclusion of the epithelium in the model, always disregarded in numerical simulations, may become relevant in the mechanical response–possibly it can justify the occurrence of corneal instabilities—after refractive surgery.

Among eye scientists, there is a diffused consciousness on the relevance of the corneal thickness on the mechanical response of the cornea, as many studies in the literature testify, including simple shell models as done in Pandolfi and Boschetti (2015). The influence of the presence of the epithelium should also be analyzed on patient-specific corneas with different corneal thickness, but this aspect was beyond the objective of this study and will be considered in future works.

Since no measurements of the epithelium stiffness have been reported in the literature, the study remains limited from the quantitative point of view. Yet, it conveys interesting results that help to reconstruct the most probable profile of the cornea stiffness across the thickness.

A final comment must be devoted to the execution times. The computational cost is affected by two reasons. Element refinement which preserves a good aspect ratio for the stroma elements increases the computational cost. The inclusion of the thin epithelium, without the corresponding exceedingly heavy refinement in the meridian section, results unavoidably in the creation of bad aspect ratio elements, which reduce the convergence rate of the explicit iterative solution procedure. The cost of the analysis grows with the refinement, with the finest mesh requiring 15 times the time of the coarsest mesh. Results reveal that the accuracy of the six-layer model is comparable to the accuracy of the nine-layer model (albeit a slight loss in terms of stresses is observed), in spite of computational times three times higher, see Table 4, last column. The adoption of a fine mesh for the evaluation of the mechanical engagement of the cornea must be decided in terms of ratio between accuracy needs and computational cost.

Appendix A: Constitutive model of the stroma

We model the stroma as a hyperelastic composite, made of an elastic matrix (made of proteoglycans) reinforced with two sets of dispersed collagen fibrils (Pandolfi and Vasta 2012). The uncertainty of the fibril orientation is described with a von Mises distribution (Pandolfi and Vasta 2012) about a main orientation $\mathbf{a}_M$, with $M = 1, 2$. The strain energy density is assumed to decompose additively into volumetric, isotropic–isochoric, and anisotropic–isochoric parts in the form

$$\Psi = \Psi_{\text{vol}}(J) + \Psi_{\text{iso}}(\bar{I}_1, \bar{I}_2) + \Psi_{\text{aniso}}(\bar{I}^*_{4M}, \sigma^2_{I_4 M}),$$

where $\mathbf{F} = d\mathbf{x}/d\mathbf{X}$ is the deformation gradient, $\mathbf{x}$ are the current coordinates and $\mathbf{X}$ the reference coordinates, and $J = \det \mathbf{F}$ is the Jacobian determinant. $\overline{\mathbf{C}} = \overline{\mathbf{F}}^T \overline{\mathbf{F}} = J^{-2/3}\mathbf{F}^T\mathbf{F}$ is the isochoric Cauchy–Green deformation tensor, and $\bar{I}_1$ and $\bar{I}_2$ are the first and the second invariants of $\overline{\mathbf{C}}$,

$$\bar{I}_1 = \text{tr}\overline{\mathbf{C}}, \qquad \bar{I}_2 = 1/2\left[(\text{tr}\overline{\mathbf{C}})^2 - \text{tr}\overline{\mathbf{C}}^2)\right],$$

where $tr(.)$ denotes the trace operator. The average pseudo-invariant $\bar{I}^*_{4M}$ is defined as

$$\bar{I}^*_{4M} = \left[\kappa_M \mathbf{I} + (1 - 3\kappa_M)\mathbf{a}_M \otimes \mathbf{a}_M\right] : \overline{\mathbf{C}}$$

where κ_M is a dispersion parameter, $\otimes$ is the tensor product, and $(:)$ is the double contraction product. The variance operator $\sigma^2_{I_4 M}$ is defined as

$$\sigma^2_{I_4 M} = \overline{\mathbf{C}} : \mathbf{a}_M \otimes \mathbf{a}_M \otimes \mathbf{a}_M \otimes \mathbf{a}_M : \overline{\mathbf{C}} - \bar{I}^*_{4M}$$

The mathematical form of the energies are

$$\Psi_{\text{vol}} = \frac{1}{4}K\left(J^2 - 1 - 2\log J\right),$$

$$\Psi_{\text{iso}} = \frac{1}{2}\left[\mu_1\left(\bar{I}_1 - 3\right) + \mu_2\left(\bar{I}_2 - 3\right)\right], \quad \mu_1 + \mu_2 = \mu,$$

$$\Psi_{\text{aniso}} = \sum_{M=1}^{2} \frac{k_{1M}}{2\,k_{2M}}\left[\exp D^*\left(\bar{I}^*_{4M}\right) - 1\right]\left(1 + K^*\sigma^2_{I_4 M}\right),$$

where K is the bulk modulus, $\mu = \mu_1 + \mu_2$ is the shear modulus of the soft isotropic matrix, while k_{1M} (stiffness-like parameter) and k_{2M} (dimensionless rigidity parameters) control the mechanical response of the reinforcing fibers at low and high strains, respectively. The coefficient $D^*(\bar{I}^*_{4M})$ reads

$$D^*\left(\bar{I}^*_{4M}\right) = k_{2M}\left(\bar{I}^*_{4M} - 1\right)^2,$$

and the coefficient K^*

$$k^* = k_{2M}\left[1 + 2D^*\left(\bar{I}^*_{4M}\right)\right].$$

The model parameters are seven: five with the dimension of a stiffness (shear elastic moduli), i.e., K, μ_1, μ_2, k_{11}, k_{12}, and two dimensionless rigidity coefficients k_{21}, k_{22}. The interested reader is referred to the original work (Pandolfi and Vasta 2012).

Acknowledgements The financial support of the iVis Technologies, Taranto, is gratefully acknowledged. A special thank goes to Giuseppe D'Ippolito and Giuseppe Criscenti. The research has been developed under the auspices of the Italian National Group of Physics–Mathematics (GNFM) of the Italian National Institution of High Mathematics "Francesco Severi" (INDAM).

References

Agca A, Ozgurhan EB, Demirok A, Bozkurt E, Celik U, Ozkaya A, Cankaya I, Yilmaz OF (2014) Comparison of corneal hysteresis and corneal resistance factor after small incision lenticule extraction and femtosecond laser-assisted lasik: a prospective fellow eye study. Contact Lens Anterior Eye 37(2):77–80

Alastrué V, Calvo B, Peña E, Doblaré M (2006) Biomechanical modeling of refractive corneal surgery. J Biomech Eng 128(1):150–160

Ariza-Gracia MÁ, Ortillés Á, Cristóbal JÁ, Rodríguez Matas JF, Calvo B (2017) A numerical-experimental protocol to characterize corneal tissue with an application to predict astigmatic keratotomy surgery. J Mech Behav Biomed Mater 74:304–314

Bongiorno T, Chojnowski JL, Lauderdale JD, Sulchek T (2016) Cellular stiffness as a novel stemness marker in the corneal limbus. Biophys J 111(8):1761–1772

Bryant MR, Marchi V, Juhasz T (2000) Mathematical models of picosecond laser in situ keratomileusis for high myopia. J Refract Surg 16:155–162

Bryant MR, McDonnell PJ (1996) Constitutive laws for biomechanical modeling of refractive surgery. J Biomech Eng

Cabrera Fernandez D, Niazy AM, Kurtz RM, Djotyan GP, Juhasz T (2005) Finite element analysis applied to cornea reshaping. J Biomed Optics 10(6):064018

Deenadayalu C, Mobasher B, Rajan SD, Hall GW (2006) Refractive change induced by the LASIK flap in a biomechanical finite element model

Elsheikh A, McMonnies CW, Whitford C, Boneham GC (2015) In vivo study of corneal responses to increased intraocular pressure loading. Eye and Vision, 2(1), All Open Access. Gold Open Access, Green Open Access

Elsheikh A, Ross S, Alhasso D, Rama P (2009) Numerical study of the effect of corneal layered structure on ocular biomechanics. Curr Eye Res 34(1):26–35

Falgayrettes N, Patoor E, Cleymand F, Zevering Y, Perone JM (2023) Biomechanics of keratoconus: two numerical studies. PLoS ONE

Jayasuriya AC, Scheinbeim JI, Lubkin V, Bennett G, Kramer P (2003) Piezoelectric and mechanical properties in bovine cornea. J Biomed Mater Res A 66A:260–265

Last JA, Liliensiek SJ, Nealey PF, Murphy CJ (2009) Determining the mechanical properties of human corneal basement membranes with atomic force microscopy. J Struct Biol 167(1):19–24

Last JA, Thomasy SM, Croasdale CR, Russell P, Murphy CJ (2012) Compliance profile of the human cornea as measured by atomic force microscopy. Micron 43(12):1293–1298

Masterton S, Ahearne M (2018) Mechanobiology of the corneal epithelium. Exp Eye Res 177:122–129

Meek KM, Boote C (2009) The use of X-ray scattering techniques to quantify the orientation and distribution of collagen in the corneal stroma. Prog Retin Eye Res 28(5):369–392

Montanino A, Angelillo M, Pandolfi A (2019) A 3d fluid-solid interaction model of the air puff test in the human cornea. J Mech Behav Biomed Mater 94:22–31

Montanino A, Gizzi A, Vasta M, Angelillo M, Pandolfi A (2018) Modeling the biomechanics of the human cornea accounting for local variations of the collagen fibril architecture. ZAMM-J Appl Math Mech /Zeitschrift für Angewandte Mathematik und Mechanik 98(12):2122–2134

Montanino A, Pandolfi A (2020) On the recovery of the stress-free configuration of the human cornea. Modell Artif Intell Ophthalmol 4:11–33

Montanino A, van Overbeeke S, Pandolfi A (2023) Modelling the biomechanics of laser corneal refractive surgery. J Mech Behavior Biomed Mater, 105998

Pandolfi A, Boschetti F (2015) The influence of the geometry of the porcine cornea on the biomechanical response of inflation tests. Comput Methods Biomech Biomed Engin 18(1):64–77

Pandolfi A, Manganiello F (2006) A model for the human cornea: constitutive formulation and numerical analysis. Biomech Model Mechanobiol 5(4):237–246

Pandolfi A, Vasta M (2012) Fiber distributed hyperelastic modeling of biological tissues. Mech Mater 44:151–162

Petsche SJ, Pinsky PM (2013) The role of 3-d collagen organization in stromal elasticity: a model based on X-ray diffraction data and second harmonic-generated images. Biomech Model Mechanobiol 12:1101–1113

Sánchez P, Moutsouris K, Pandolfi A (2014) Biomechanical and optical behavior of human corneas before and after photorefractive keratectomy. J Cataract Refract Surg 40(6):905–917

Seven I, Vahdati A, Pedersen IB, Vestergaard A, Hjortdal J, Roberts CJ, Dupps WJ (2017) Contralateral eye comparison of smile and flap-based corneal refractive surgery: computational analysis of biomechanical impact. J Refract Surg 33(7):444–453

Simonini I, Pandolfi A (2015) Customized finite element modelling of the human cornea. PLoS ONE 10(6):e0130426

Sinha-Roy A, Dupps WJ (2009) Effects of altered corneal stiffness on native and postoperative LASIK corneal biomechanical behavior: a whole-eye finite element analysis. J Refract Surg 25(10):875–887

Sinha-Roy A, Dupps W. J (2011) Patient-specific modeling of corneal refractive surgery outcomes and inverse estimation of elastic property changes. J Biomech Eng, 133(1),

Sinha-Roy A, Dupps WJ, Roberts CJ (2014) Comparison of biomechanical effects of small-incision lenticule extraction and laser in situ keratomileusis: finite-element analysis. J Cataract Refract Surg 40(6):971–980

Straehla JP, Limpoco FT, Dolgova NV, Keselowsky BG, Sawyer WG, Perry SS (2010) Nanomechanical probes of single corneal epithelial cells: shear stress and elastic modulus. Tribol Lett 38:107–113

Studer HP, Riedwyl H, Amstutz CA, Hanson James VM, Büchler P (2013) Patient-specific finite-element simulation of the human cornea: a clinical validation study on cataract surgery. J Biomech 46(4):751–758

Thomasy SM, Raghunathan VK, Winkler M, Reilly CM, Sadeli AR, Russell P, Jester JV, Murphy CJ (2014) Elastic modulus and collagen organization of the rabbit cornea: epithelium to endothelium. Acta Biomater 10(2):785–791

Torres-Netto EA, Hafezi F, Spiru B, Gilardoni F, Hafezi NL, Gomes JAP, Randleman JB, Sekundo W, Kling S (2021) Contribution of bowman layer to corneal biomechanics. J Cataract Refract Surg 47(7):927–932

Whitford C, Studer H, Boote C, Meek KM, Elsheikh A (2015) Biomechanical model of the human cornea: considering shear stiffness and regional variation of collagen anisotropy and density. J Mech Behav Biomed Mater 42:76–87